Frequency Dependence of Resonance Field of One-Dimensional Heisenberg Antiferromagnet $KCuF_3$ *

SHI Qing-Fan(史庆藩)[1**], LÜ Zhen(吕震)[1], MA Mu-Yan(马牧燕)[2], MA Chao(马超)[1], LI Liang-Sheng(李粮生)[1]

[1] *Department of Physics, Faculty of Science, Beijing Institute of Technology, Beijing 100081*
[2] *Department of Electric Engineering, Beijing Institute of Machinery, Beijing 100085*

(Received 1 December 2005)

The frequency dependence of the in-plane angular change of the antiferromagnetic resonance (AFMR) field of $KCuF_3$ is systematically measured at frequencies ranging from 3.8 to 10.6 GHz at 4.2 K. The effect of inequivalent g-tensors is found to gradually diminish with decreasing the frequency, and completely vanish when the frequency is decreased to the lower-frequency branch of C-band, while the effect of the effective anisotropy field is significantly enhanced with decreasing the frequency. The calculated AFMR field $\boldsymbol{H}_{\rm res}$ based on the eight-sublattice model proposed by Yamada and Kato [J. Phys. Soc. Jpn. 63 (1994) 289] is in good agreement with the experimental data.

PACS: 75. 50. Ee, 75. 25. +z, 75. 30. Gw

The magnetic properties of the ferro- and antiferromagnetic materials have received enormous attention in the past decade due to their industrial applications, such as magnetic storage, antiferromagnetically-coupled media, medical imaging and superconductors. The research for one-dimensional Heisenberg antiferromagnet $KCuF_3$ is a typical example.[1−8] Besides the theoretical research, the resonance method is one of the important technique for providing the evidence of the magnetic structure. In the previous magnetic resonance experiments,[5−9] many characteristics of this compound have been discovered, e.g., the linear antiferromagnetic chains of $KCuF_3$ is known to be along the c-axis with the intrachain exchange interaction $J_c = -190\,\mathrm{K}$, and the very weak interchain exchange interaction in the c-plane estimated to be $J_a \simeq 0.01|J_c|$ at temperatures below $T_N = 39\,\mathrm{K}$; the substantial easy direction is along $[110]_p$ and its equivalent axes, where $[\ ]_p$ represents an axis in a unit cell of a perovskite structure. In particular, an eight-sublattice magnetic structure of $KCuF_3$ was first proposed according to the observation of the four-fold symmetric change of antiferromagnetic resonance (AFMR) field $\boldsymbol{H}_{\rm res}$ in the c-plane at 9.1 GHz using an X-band spectrometer.[10] Furthermore, the analysis of the in-plane angular change of $\boldsymbol{H}_{\rm res}$ respectively operated at 9.1 and 23.4 GHz for various temperatures concludes that the two larger peaks appearing at $\boldsymbol{H}//[100]_p$ and its equivalent direction $[010]_p$ are caused by the effective anisotropy field produced by the Dzyaloshinsky–Moriya (DM) antisymetric exchange interaction $\sum_{i>j} d_{ij} \cdot (\boldsymbol{S}_i \times \boldsymbol{S}_j)$, whereas the two smaller peaks at $\boldsymbol{H}//[110]_p$ are due to the effect of the inequivalent $\boldsymbol{g}$-tensors.[10−15] Accordingly, instead of solving the equations of motion to elucidate the effect of inequivalent g-tensors, antiferromagnetic resonance (AFMR) of this compound should reflect the frequency dependency of the effect of both effective anisotropy and inequivalent $\boldsymbol{g}$-tensor. However, previous AFMR experiments leading to the above conclusions were conducted only on the two kinds of resonance modes, e.g., 9.1 and 23.4 GHz, the frequency dependence of the in-plane angular change of the AFMR field $\boldsymbol{H}_{\rm res}$ is still not systematically investigated. Therefore, in order to fully clarify the characteristic of $KCuF_3$, the AFMR at other frequencies should also be carried out. In this Letter, we concentrate on how the effects of both the inequivalent $\boldsymbol{g}$-tensors and the DM interaction are related to the changing resonance frequency. The data of AFMR experiments is compared with the calculation based on the eight-sublattice model proposed by Yamada and Kato,[10] so as to confirm the correctness of the postulation of magnetic structure.

The $KCuF_3$ single crystal used in the present experiment has high quality and has ever been used in previously studies.[10−12] AFMR measurements are performed at various frequencies ranging from 3.8 to 10.6 GHz and 4.2 K, far below $T_N = 39\,\mathrm{K}$. A wide-band spectrometer operated from 2 GHz to 20 GHz is employed to investigate the angular dependence of $\boldsymbol{H}_{\rm res}$. The sample is placed at the bottom centre of a TE_{101} rectangle cavity and a water-cooled magnet rotates around the vertical axis by a rotation mechanism. In order to obtain the different resonance frequencies, the cavity is lengthened and filled with different quantities of Teflon materials.

When the external field $\boldsymbol{H}$ is rotated in the c-

* Supported by the Ministry of Education of China for Returned Overseas Scholars under Grant No LQ2000-2.
** Email: qfshi@163.com
©2006 Chinese Physical Society and IOP Publishing Ltd

plane, the changes of the resonance field $\boldsymbol{H}_{\rm res}$ in higher-frequency branch ($f > 5$ GHz) shows a four-fold symmetry as displayed by the solid circles in Figs. 1(a)–1(d), where two larger peaks of $\boldsymbol{H}_{\rm res}$ appear at $\boldsymbol{H}//[100]_p$ and its equivalent direction $[010]_p$, whereas two smaller peaks appear at $\boldsymbol{H}//[110]_p$ directions. This result is similar to that observed in the previous AFMR experiment at 9.1 GHz.[10] On the other hand, when the resonance frequency is decreased to the lower-frequency branch ($f < 5$ GHz), the resonance $\boldsymbol{H}_{\rm res}$ of the in-plane angular change of AFMR behaves typically as those shown in Figs. 1(e)–1(f), where only two large peaks of AFMR appear at $\boldsymbol{H}//[100]_p$ and its equivalent direction $[010]_p$, and seem to be more spiky in shape than those observed at higher frequencies, and no peak occurs at $\boldsymbol{H}//[110]_p$. Taken together for all frequencies shown in Fig. 1, heights of the peaks at $\boldsymbol{H}//[110]_p$ appear to gradually degenerate as frequency decreases. In contrast, a difference between the peak at $\boldsymbol{H}//[100]_p$ and the peak at $\boldsymbol{H}//[110]_p$ significantly grow as frequency decreases. Note that the peaks appearing at $\boldsymbol{H}//[100]_p$ and its equivalent direction $[010]_p$ have been identified to be caused by the effective anisotropy field produced by the DM interaction, and the peaks at $\boldsymbol{H}//[110]_p$ by the effect of the inequivalent g-tensors.[10–12] Thus, the effect of inequivalent g-tensors gradually diminishes with decreasing the frequency, and completely vanishes as the frequency is decreased to the lower-frequency branch of C-band, while the effect of the effective anisotropy field is significantly enhanced with decreasing the frequency. Moreover, the ratio of the resonance fields along the directions of $[110]_p$ and $[100]_p$ is reviewed and depicted in the inset of Fig. 2. It can be easily observed that the resonance fields along the two directions is equivalent at about 11.7 GHz from the fitting line of the experimental data. In fact, $\boldsymbol{H}_{\rm res}$ observed at 23.4 GHz in the c-plane behaves only two large peaks at $\boldsymbol{H}//[110]_p$, and no corresponding peaks appear at $\boldsymbol{H}//[100]_p$ and its equivalent direction, i.e., $\boldsymbol{H}_{\rm res}$ at $[110]_p$ becomes larger than $\boldsymbol{H}_{\rm res}$ at $[100]_p$ when the resonance frequency exceeds 11.7 GHz. In addition, the second absorption represented by the hollow square in Fig. 1 is observed to exist in the substantial uneasy direction of the spin $[100]_p$ axis at the lower-frequencies, to which the details will be published elsewhere. The experimental diagram of the resonance frequency-field is shown in Fig. 2, in which the solid circle is for $\boldsymbol{H}//[110]_p$, the square for $\boldsymbol{H}//[100]_p$, and the hollow square is for the second absorption at $\boldsymbol{H}//[100]_p$.

Now we calculate the frequency dependence of $\boldsymbol{H}_{\rm res}$ in light of the eight sublattices model proposed by Yamada and Kato.[10] According to the conventional AFMR theory, the Hamiltonian is written as

$$\begin{aligned}\hat{H} = & -2\sum_{i>j}(J_c\boldsymbol{S}_i\cdot\boldsymbol{S}_j + D_c\boldsymbol{S}_i^z\cdot\boldsymbol{S}_j^z) \\ & -2\sum_{i>m}J_a\boldsymbol{S}_l\cdot\boldsymbol{S}_m + \sum_{i>j}d_{ij}\cdot(\boldsymbol{S}_i\times\boldsymbol{S}_j) \\ & +\mu_B\sum_k\boldsymbol{S}_k\cdot\boldsymbol{g}_A\cdot\boldsymbol{H} + \mu_B\sum_{k'}\boldsymbol{S}_{k'}\cdot\boldsymbol{g}_B\cdot\boldsymbol{H},\end{aligned} \tag{1}$$

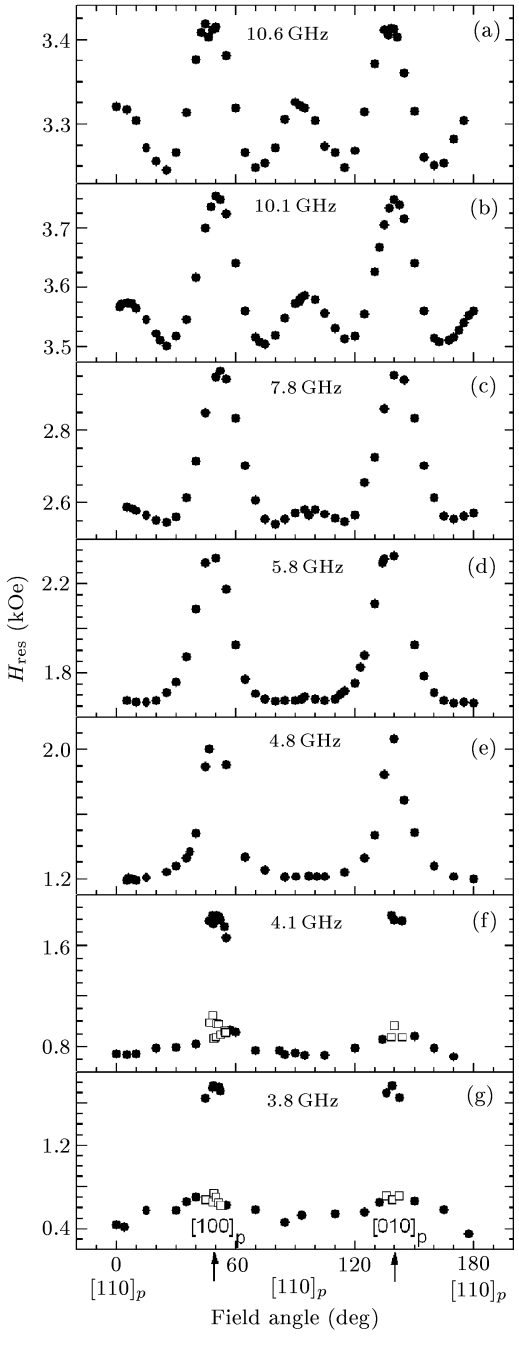

Fig. 1. The angular dependence of the in-plane resonance field $\boldsymbol{H}_{\rm res}$ observed at 4.2 K under various frequencies when the direction of the external field $\boldsymbol{H}$ is rotated in the c-plane. The solid circle represents the main resonance absorption, and the hollow square denote the second weaker absorption.

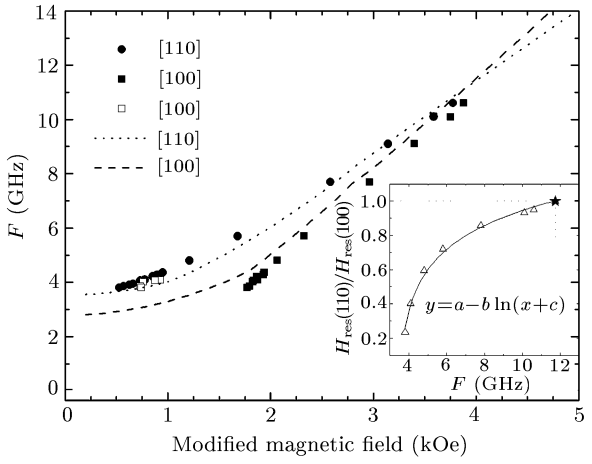

Fig. 2. Frequency-field diagram. The solid circle is for $\boldsymbol{H}//[110]_p$, the solid square for $\boldsymbol{H}//[100]_p$, the hollow square for the second absorption at $\boldsymbol{H}//[100]_p$. The abscissa is the modified field $\boldsymbol{H} \equiv |\boldsymbol{g}_m \cdot \boldsymbol{H}/g|$ where g is the g-value of a free electron and $\boldsymbol{g}_m \equiv (\boldsymbol{g}_A + \boldsymbol{g}_B)/2$. The calculated results are described by the dotted line for $\boldsymbol{H}//[110]_p$, the dashed line for $\boldsymbol{H}//[100]_p$. Each triangle in the inset means the ratio of the resonance fields along the directions of $[110]_p$ and $[100]_p$ for one fixed frequency. The solid line is only the fitting curve. The star represents the experimentally predicted equivalence point of the resonance fields along $[110]_p$ and $[100]_p$.

where J_c represents the intrachain exchange interactions among the nearest-neighbouring ions in the c-axis, J_a means the ferromagnetic interchain exchange interaction among nn ions in the c-plane, and $D_c = 0.04\,\mathrm{K}$ produces an XY-like anisotropy field which forces the spins to lie in the c-plane.[16] The third term represents the DM interaction between nn spins in the c-axis, which can be denoted as $\boldsymbol{H}_{\mathrm{DM}}$. The last two terms are the Zeeman interactions for the spins having inequivalent $\boldsymbol{g}$-tensors, $\boldsymbol{g}_A$ and $\boldsymbol{g}_B$, where the two summations $\sum_k$ and $\sum_{k'}$ represent the spins having $\boldsymbol{g}_A$ and $\boldsymbol{g}_B$, respectively. Because of the DM interaction and the inequivalent $\boldsymbol{g}$-tensors, the spins are canted and divided into eight sublattices. The equations of motion of eight-sublattice can be written as follows:

$$\frac{d\boldsymbol{M}_{i\alpha}}{dt} = -\gamma[\boldsymbol{M}_i \times \boldsymbol{H}_i], \quad (i = 1\text{–}8, \text{ and } \alpha = x, y, z), \tag{2}$$

with

$$\boldsymbol{M}_i = \boldsymbol{M}_{i0} + \boldsymbol{m}_i,$$
$$\boldsymbol{H}_i = \boldsymbol{H}_{i0} + \boldsymbol{h}_i,$$

where $\gamma = -g\mu_B/\hbar$; $\boldsymbol{M}_{i0}$ and $\boldsymbol{H}_{i0}$ are the steady parts of the sublattice magnetization and mean field, respectively; $\boldsymbol{m}_i$ and $\boldsymbol{h}_i$ represent the parts containing $\exp(i\omega t)$ in $\boldsymbol{M}_i$ and $\boldsymbol{H}_i$, respectively. Thus, the resonance frequencies should be the eigenvalues of the matrix with 24×24 elements. From the expressions of Hamiltonian and the mean field $\boldsymbol{H}_i$ acting on the sublattice magnetization $\boldsymbol{M}_i$, we have

$$\begin{aligned}
\boldsymbol{H}_1 =& \frac{\boldsymbol{g}_A}{g} \cdot \boldsymbol{H} - A\boldsymbol{M}_5 + A'(\boldsymbol{M}_2 + \boldsymbol{M}_4) \\
& - B(\boldsymbol{M}_5 + \boldsymbol{d}_{15}) + \boldsymbol{H}_{A1}, \\
\boldsymbol{H}_2 =& \frac{\boldsymbol{g}_B}{g} \cdot \boldsymbol{H} - A\boldsymbol{M}_6 + A'(\boldsymbol{M}_1 + \boldsymbol{M}_3) \\
& - B(\boldsymbol{M}_6 \times \boldsymbol{d}_{26}) + \boldsymbol{H}_{A2}, \\
\boldsymbol{H}_3 =& \frac{\boldsymbol{g}_A}{g} \cdot \boldsymbol{H} - A\boldsymbol{M}_7 + A'(\boldsymbol{M}_2 + \boldsymbol{M}_4) \\
& - B(\boldsymbol{M}_7 \times \boldsymbol{d}_{37}) + \boldsymbol{H}_{A3}, \\
\boldsymbol{H}_4 =& \frac{\boldsymbol{g}_B}{g} \cdot \boldsymbol{H} - A\boldsymbol{M}_8 + A'(\boldsymbol{M}_1 + \boldsymbol{M}_3) \\
& - B(\boldsymbol{M}_8 \times \boldsymbol{d}_{48}) + \boldsymbol{H}_{A4}, \\
\boldsymbol{H}_5 =& \frac{\boldsymbol{g}_A}{g} \cdot \boldsymbol{H} - A\boldsymbol{M}_1 + A'(\boldsymbol{M}_6 + \boldsymbol{M}_8) \\
& - B(\boldsymbol{M}_1 \times \boldsymbol{d}_{15}) + \boldsymbol{H}_{A5}, \\
\boldsymbol{H}_6 =& \frac{\boldsymbol{g}_B}{g} \cdot \boldsymbol{H} - A\boldsymbol{M}_2 + A'(\boldsymbol{M}_5 + \boldsymbol{M}_7) \\
& - B(\boldsymbol{M}_2 \times \boldsymbol{d}_{26}) + \boldsymbol{H}_{A6}, \\
\boldsymbol{H}_7 =& \frac{\boldsymbol{g}_A}{g} \cdot \boldsymbol{H} - A\boldsymbol{M}_3 + A'(\boldsymbol{M}_6 + \boldsymbol{M}_8) \\
& - B(\boldsymbol{M}_3 \times \boldsymbol{d}_{37}) + \boldsymbol{H}_{A7}, \\
\boldsymbol{H}_8 =& \frac{\boldsymbol{g}_B}{g} \cdot \boldsymbol{H} - A\boldsymbol{M}_4 + A'(\boldsymbol{M}_5 + \boldsymbol{M}_7) \\
& - B(\boldsymbol{M}_4 \times \boldsymbol{d}_{48}) + \boldsymbol{H}_{A8},
\end{aligned} \tag{3}$$

where the first terms on the right-hand side are the external fields respectively modified by $\boldsymbol{g}_A$ and $\boldsymbol{g}_B$; the second and third terms respectively correspond to the exchange field from J_c and J_a; the fourth terms come from the DM interaction characterized by the following vector $\boldsymbol{d}_{ij}$:

$$\begin{aligned}
\boldsymbol{d}_{15} &= \boldsymbol{d}_{73} = [-d, 0, 0], \\
\boldsymbol{d}_{51} &= \boldsymbol{d}_{37} = [d, 0, 0], \\
\boldsymbol{d}_{26} &= \boldsymbol{d}_{84} = [0, -d, 0], \\
\boldsymbol{d}_{48} &= \boldsymbol{d}_{62} = [0, d, 0];
\end{aligned}$$

and the last terms represent the XY-like anisotropy field. $M_i = -Ng\mu_B\langle S_i\rangle$ $(i = 1 \sim 8)$ is the magnetization of the ith sublattice, in which N is the number of magnetic ions in the ith sublattice, g is the g-factor of a free electron, and $\langle\ \rangle$ a thermal average. The coordinate system $[x, y, z]$ is taken to be parallel to the $[100]_p$, $[010]_p$ and $[001]_p$ axes, respectively.

Because of the difficulty of analytically solving such a large-scale system of equations, equations (2) of motion are numerically calculated to obtain the eigen frequencies. In the calculation, the experimental data $J_c = -190\,\mathrm{K}$, $J_a = 0.01|J_c|$, $D_c = 0.04\,\mathrm{K}$,[4,16] and $d = 0.027|J_c|$ are used. The parameters in Eq. (2) are determined by

$$A = \frac{4|J_c|}{N\gamma^2\hbar^2}, \quad A' = \frac{4J_a}{N\gamma^2\hbar^2},$$

$$B = \frac{4}{N\gamma^2 h^2}, \quad K = \frac{4D_c}{N\gamma^2 h^2}, \tag{4}$$

where $\gamma = -g\mu_B/\hbar$. Moreover, the first approximation

$$\boldsymbol{M}_{i0} \times \boldsymbol{H}_{i0} = 0$$

is also used as the initial condition, and therefore we can obtain the linear equations of motion

$$\frac{i\omega}{\gamma}\boldsymbol{m}_i + \boldsymbol{m}_i \times \boldsymbol{H}_{i0} + \boldsymbol{M}_{i0} \times \boldsymbol{h}_i = 0, \quad (i = 1\text{–}8). \tag{5}$$

The calculated frequency-field diagram for the lowest-frequency mode is shown in Fig. 2, in which the dashed line is for $\boldsymbol{H}//[100]_p$, the dotted line for $\boldsymbol{H}//[110]_p$. Obviously, the calculated AFMR field $\boldsymbol{H}_{\rm res}$ is in good agreement with the data of AFMR experiments.

In conclusion, the antiferromagnetic resonance method experimentally find that the effect of inequivalent g-tensors in $KCuF_3$ gradually degenerates with decreasing the frequency, and completely vanishes when the frequency is decreased to the lower-frequency branch of C-band, while the effect of the effective anisotropy field arising from the DM interaction is significantly enhanced with decreasing the frequency. The fact that the calculated diagram of $\boldsymbol{H}_{\rm res}$ at the directions of both $[100]_p$ and $[110]_p$ is in good agreement with the data of experiments reconfirms the eight-sublattice structure of $KCuF_3$. Our results provide valuable reference for the potential applications of this kind of compounds.

We are very grateful to M. Mino, H. Yamazaki and I. Yamada for their invaluable support.

References

[1] Liu W and Zhou B 1995 *Chin. Phys. Lett.* **12** 106
[2] Huang C, Wang H and Wang E 2003 *Chin. Phys. Lett.* **20** 1593
[3] Ekrem Aydiner and Cenk Akyüz 2005 *Chin. Phys. Lett.* **22** 2382
[4] Kadota S, Yamada I, Yoneyyama S and Hirakawa K 1967 *J. Phys. Soc. Jpn.* **22** 751
[5] Ikebe M and Date M 1971 *J. Phys. Soc. Jpn.* **30** 93
[6] Hutchings M T, Samuelsen E J, Shirane G and Hirakawa K 1969 *Phys. Rev.* **188** 919
[7] Kubo H, Tanaka F, Kaneshima N and Hirakawa K 1976 *Solid State Commun.* **18** 79
[8] Yamada I, Fujii H and Hidala M 1989 *J. Phys.: Condens. Matter* **1** 3397
[9] Ishii T and Yamada I 1990 *J. Phys.: Condens. Matter* **2** 5771
[10] Yamada I and Kato N 1994 *J. Phys. Soc. Jpn.* **63** 289
[11] Kato N and Yamada I 1994 *J. Phys. Soc. Jpn.* **63** 3515
[12] Sasaki S, Narita N and Yamada I 1995 *J. Phys. Soc. Jpn.* **64** 4882
[13] Hidaka M, Eguchi T and Yamada I 1998 *J. Phys. Soc. Jpn.* **67** 2488
[14] Dzyaloshinsky I 1958 *J. Phys. Chem. Solids* **4** 241
[15] Moriya T 1960 *Phys. Rev.* **120** 91
[16] Satija S K, Axe J D, Shirane G, Yoshizawa H and Hirakawa K 1980 *Phys. Rev.* B **21** 2001